Gradient Shape-Persistent π-Conjugated Dendrimers for Light-Harvesting: Synthesis, Photophysical Properties, and Energy Funneling

ARTICLE *in* JOURNAL OF THE AMERICAN CHEMICAL SOCIETY · AUGUST 2008

Impact Factor: 12.11 · DOI: 10.1021/ja803109r · Source: PubMed

6 AUTHORS, INCLUDING:

Qi Xiao
University of Pennsylvania
9 PUBLICATIONS **194** CITATIONS
SEE PROFILE

Yuguo Ma
Peking University
71 PUBLICATIONS **1,637** CITATIONS
SEE PROFILE

Article

Gradient Shape-Persistent #-Conjugated Dendrimers for Light-Harvesting: Synthesis, Photophysical Properties, and Energy Funneling

Jin-Liang Wang, Jing Yan, Zheng-Ming Tang, Qi Xiao, Yuguo Ma, and Jian Pei

J. Am. Chem. Soc., **2008**, 130 (30), 9952-9962 • DOI: 10.1021/ja803109r • Publication Date (Web): 01 July 2008

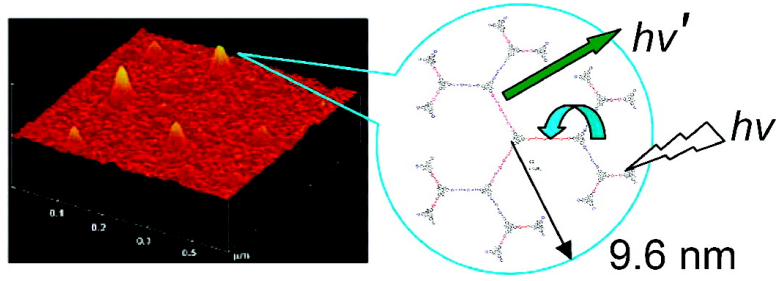

More About This Article

Additional resources and features associated with this article are available within the HTML version:

- Supporting Information
- Links to the 1 articles that cite this article, as of the time of this article download
- Access to high resolution figures
- Links to articles and content related to this article
- Copyright permission to reproduce figures and/or text from this article

View the Full Text HTML

J|A|C|S
ARTICLES

Published on Web 07/01/2008

Gradient Shape-Persistent π-Conjugated Dendrimers for Light-Harvesting: Synthesis, Photophysical Properties, and Energy Funneling

Jin-Liang Wang, Jing Yan, Zheng-Ming Tang, Qi Xiao, Yuguo Ma,* and Jian Pei*

Beijing National Laboratory for Molecular Sciences, Key Laboratories of Bioorganic Chemistry and Molecular Engineering and Polymer Chemistry and Physics of Ministry of Education, College of Chemistry, Peking University, Beijing 100871, China

Received April 27, 2008; E-mail: jianpei@pku.edu.cn

Abstract: A new class of π-conjugated dendrimers **G0**, **G1**, and **G2** was developed through a double-stage divergent/convergent growth approach, in which 5,5,10,10,15,15-hexahexyltruxene was employed as the node and oligo(thienylethynylene)s (OTEs) with different lengths as the branching moieties. The dendrimers were fully characterized by ^{1}H and ^{13}C NMR, elemental analysis, gel permeation chromatography, and MALDI-TOF MS. Also, by using atomic force microscopy, it was observed that dendrimer **G2** laid nearly flat on the mica surface as a single molecule. Dynamic light scattering results showed that the molecule retained its relatively flat shape in solution. To our best knowledge, dendrimer **G2**, with a radius approaching 10 nm and a molecular weight of 27 072 Da, was the largest among reported second generation dendrimers. The energy gradient in **G2** was constructed by linking OTEs of increasing effective conjugation lengths from the dendritic rim to the core. The intramolecular energy transfer process was studied using steady-state UV−vis absorption and photoluminescent spectroscopies, as well as time-resolved fluorescence spectroscopy. Our structurally extended dendrimers showed an excellent energy funneling ability (their energy transfer efficiencies were all over 95%). All results demonstrate that these dendrimers are promising candidates as light-harvesting materials for optoelectronic devices.

Introduction

π-Conjugated dendrimers represent a new class of shape-persistent macromolecular materials of well-defined structures and have shown great application potentials in electronic and optoelectronic devices,[1] such as organic field-effect transistors (OFETs),[2] electroluminescent devices,[3] and solar cells.[4] To overcome the steric crowdedness in the synthesis of higher generation dendrimers, a gradient of the branch lengths can be

(1) (a) Miller, T. M.; Neenan, T. X.; Zayas, R.; Bair, H. E. *J. Am. Chem. Soc.* **1992**, *114*, 1018–1025. (b) Xu, Z.; Moore, J. S. *Angew. Chem., Int. Ed. Engl.* **1993**, *32*, 246–248. (c) Xu, Z.; Kahr, M.; Walker, K. L.; Wilkins, C. L.; Moore, J. S. *J. Am. Chem. Soc.* **1994**, *116*, 4537–4550. (d) Deb, S. K.; Maddux, T. M.; Yu, L. *J. Am. Chem. Soc.* **1997**, *119*, 9079–9080. (e) Meier, H.; Lehmann, M. *Angew. Chem., Int. Ed.* **1998**, *37*, 643–645. (f) Pillow, J. N. G.; Halim, M.; Lupton, J. M.; Burn, P. L.; Samuel, I. D. W. *Macromolecules* **1999**, *32*, 5985–5993. (g) Berresheim, A. J.; Müller, M.; Müllen, K. *Chem. Rev.* **1999**, *99*, 1747–1787. (h) Grayson, S. M.; Fréchet, J. M. J. *Chem. Rev.* **2001**, *101*, 3819–3867. (i) Lupton, J. M.; Samuel, I. D. W.; Beavington, R.; Burn, P. L.; Bässler, H. *Adv. Mater.* **2001**, *13*, 258–261. (j) Yamamoto, K.; Higuchi, M.; Shiki, S.; Tsuruta, M.; Chiba, H. *Nature (London, U.K.)* **2002**, *415*, 509–511. (k) Imaoka, T.; Horiguchi, H.; Yamamoto, K. *J. Am. Chem. Soc.* **2003**, *125*, 340–341. (l) McClenaghan, N. D.; Passalacqua, R.; Loiseau, F.; Campagna, S.; Verheyde, B.; Hameurlaine, A.; Dehaen, W. *J. Am. Chem. Soc.* **2003**, *125*, 5356–5365. (m) Cao, X.-Y.; Zhang, W.-B.; Wang, J.-L.; Zhou, X.-H.; Lu, H.; Pei, J. *J. Am. Chem. Soc.* **2003**, *125*, 12430–12431. (n) Díez-Barra, E.; García-Martínez, J. C.; Rodríguez-López, J. *J. Org. Chem.* **2003**, *68*, 832–838. (o) Simpson, C. D.; Mattersteig, G.; Martin, K.; Gherghel, L.; Bauer, R. E.; Räder, H. J.; Müllen, K. *J. Am. Chem. Soc.* **2004**, *126*, 3139–3147. (p) Shen, X.; Ho, D. M.; Pascal, R. A., Jr. *J. Am. Chem. Soc.* **2004**, *126*, 5798–5805. (q) Xia, C.; Fan, X.; Locklin, J.; Advincula, R. C.; Gies, A.; Nonidez, W. *J. Am. Chem. Soc.* **2004**, *126*, 8735–8743. (r) Loiseau, F.; Campagna, S.; Hameurlaine, A.; Dehaen, W. *J. Am. Chem. Soc.* **2005**, *127*, 11352–11363. (s) Hwang, G. T.; Kim, B. H. *Org. Lett.* **2004**, *6*, 2669–2672. (t) Yang, J.-X.; Tao, X.-T.; Yuan, C.-X.; Yan, Y.-X.; Wang, L.; Liu, Z.; Ren, Y.; Jiang, M. H. *J. Am. Chem. Soc.* **2005**, *127*, 3278–3279. (u) Bernhardt, S.; Kastler, M.; Enkelmann, V.; Baumgarten, M.; Müllen, K. *Chem.—Eur. J.* **2006**, *12*, 6117–6128. (v) Itami, K.; Tonogaki, K.; Nokami, T.; Ohashi, Y.; Yoshida, J.-i. *Angew. Chem., Int. Ed.* **2006**, *45*, 2404–2409. (w) Oesterling, I.; Müllen, K. *J. Am. Chem. Soc.* **2007**, *129*, 4595–4605. (x) Lawrence, J. R.; Namdas, E. B.; Richards, G. J.; Burn, P. L.; Samuel, I. D. W. *Adv. Mater.* **2007**, *19*, 3000–3003. (y) Varnavski, O.; Yan, X.; Mongin, O.; Blanchard-Desce, M.; Goodson, T., III *J. Phys. Chem. C* **2007**, *111*, 149–162. (z) Rajadurai, M. S.; Shifrina, Z. B.; Kuchkina, N. V.; Rusanov, A. L.; Müllen, K. *Russ. Chem. Rev.* **2007**, *76*, 767–783.

(2) (a) Negishi, N.; Ie, Y.; Taniguchi, M.; Kawai, T.; Tada, H.; Kaneda, T.; Aso, Y. *Org. Lett.* **2007**, *9*, 829–832. (b) Kim, K. H.; Chi, Z.; Cho, M. J.; Jin, J-I.; Choi, D. H.; Paek, S. H. *Macromol. Symp.* **2007**, *249−250*, 1–7.

(3) (a) Wang, P. W.; Liu, Y.-J.; Devadoss, C.; Bharathi, P.; Moore, J. S. *Adv. Mater.* **1996**, *8*, 237–241. (b) Halim, M.; Pillow, J. N. G.; Samuel, I. D. W.; Burn, P. L. *Adv. Mater.* **1999**, *11*, 371–374. (c) Lupton, J. M.; Samuel, I. D.W.; Frampton, M. J.; Beavington, R.; Burn, P. L. *Adv. Funct. Mater.* **2001**, *11*, 287–294. (d) Ma, D.; Lupton, J. M.; Beavington, R.; Burn, P. L.; Samuel, I. D. W. *Adv. Funct. Mater.* **2002**, *12*, 507–511. (e) Satoh, N.; Cho, J.-S.; Higuchi, M.; Yamamoto, K. *J. Am. Chem. Soc.* **2003**, *125*, 8104–8105. (f) Cao, X.-Y.; Liu, X.-H.; Zhou, X.-H.; Zhang, Y.; Jiang, Y.; Cao, Y.; Cui, Y.-X.; Pei, J. *J. Org. Chem.* **2004**, *69*, 6050–6058. (g) Kwon, T. W.; Alam, M. M.; Jenekhe, S. A. *Chem. Mater.* **2004**, *16*, 4657–4666. (h) Kimoto, A.; Cho, J.-S.; Higuchi, M.; Yamamoto, K. *Macromolecules* **2004**, *37*, 5531–5537. (i) Loiseau, F.; Campagna, S.; Hameurlaine, A.; Dehaen, W. *J. Am. Chem. Soc.* **2005**, *127*, 11352–11363. (j) Zhao, L.; Li, C.; Zhang, Y.; Zhu, X.-H.; Peng, J.; Cao, Y. *Macromol. Rapid Commun.* **2006**, *27*, 914–920.

10.1021/ja803109r CCC: $40.75

introduced into the dendrimer scaffold to reduce the steric hindrance at the periphery as well as to increase the volume of the interior.[5] In practice, this would lead to dendrimers with an expanded molecular architecture that differ greatly from the traditional, more compact dendrimers. This unique and interesting molecular architecture may have significant consequences on the properties of the dendrimers, as well as their performances in electronic and optoelectronic devices.

At the same time, light-absorbing dendritic branches can be incorporated into the π-conjugated dendrimer scaffold to achieve high molar extinction coefficients in a broad absorption region,[6] making such dendrimers promising candidates for light-harvesting materials. In the highly efficient photosynthetic process in nature, the energy of sunlight was first collected and then converted into chemical energy through a series of photophysical and photochemical process. It is shown that in some natural photosynthetic systems, the exciton initially generated at the periphery can be funneled rapidly and unidirectionally to the reaction center through a continuous energy gradient.[7] To mimic the natural photosynthetic process, an energy gradient could be constructed into the dendrimer backbones to achieve directional energy flow from the peripheral branches to the core.[8] Indeed, several examples of conjugated dendrimers and dendrons have exhibited efficient and unidirectional energy transfer properties, in which the importance of the energy gradient was highlighted.[9]

To put the previous ideas into practice, suitable dendrimer scaffold should be carefully chosen. We identified several criteria for ideal branches in such dendrimers: (1) easily tunable lengths through a facile chemical synthesis approach; (2) linear, rigid structures with a minimum conformational flexibility; and (3) tunable absorption and emission behaviors. An extensive literature survey brought oligo(thienylethynylene)s (OTEs) to our attention. OTEs have attracted considerable research interest due to their rigid geometry and ability to effectively transfer energy over long distances.[10] The excellent optical and electronic properties of OTEs as well as their structural rigidity make them ideal candidates for branching units in constructing shape-persistent dendrimers.[11]

In our previous contributions, 5,5,10,10,15,15-hexahexyltruxene exhibited several features as an excellent node in such light-harvesting dendrimers. Minimum electronic communication between chromophores attached to the different sides of the truxene unit ensures the independence of individual chromophores, which greatly simplifies the interpretation of the photophysical process.[12] Moreover, the multiple hexyl groups effectively improve the solubility of the designed dendrimer in common organic solvents, a main obstacle usually encountered in synthesizing and characterizing such rigid conjugated molecules. As an extension of our work on dendrimers solely constructed with 5,5,10,10,15,15-hexahexyltruxene units, we developed a series of dendrimers **G0** and **G1** (Chart 1), using OTEs with different lengths as branching units.[13] As a step further, we made a supersized π-conjugated dendrimer **G2** as shown in Chart 2, which contains 22 5,5,10,10,15,15-hexahexyltruxene building blocks as the nodes and OTE units with different conjugation lengths as the branches. To the best of our knowledge, dendrimer **G2** features the largest diameter and the highest molecular weight among all reported second generation dendrimers. The energy gradient within **G2** is engineered by linking OTE units of increasing length from the dendritic rim to the core, which at the same time reduces congestion around the dendrimer periphery at higher generations. Such an energy gradient, combined with the proximity of chromophores in such a structural framework, is ideal for an efficient energy transfer process within our supersized, extended

(4) (a) Satoh, N.; Nakashima, T.; Yamamoto, K. *J. Am. Chem. Soc.* **2005**, *127*, 13030–13038. (b) Petrella, A.; Cremer, J.; De Cola, L.; Bäuerle, P.; Williams, R. M. *J. Phys. Chem. A* **2005**, *109*, 11687–11695. (c) Kopidakis, N.; Mitchell, W. J.; van de Lagemaat, J.; Ginley, D. S.; Rumbles, G.; Shaheen, S. E. *Appl. Phys. Lett.* **2006**, *89*, 103504. (d) Cremer, J.; Bäuerle, P. *J. Mater. Chem.* **2006**, *16*, 874–884. (e) Lu, J.; Xia, P. F.; Lo, P. K.; Tao, Y.; Wong, M. S. *Chem. Mater.* **2006**, *18*, 6194–6203. (f) Ma, C.-Q.; Mena-Osteritz, E.; Debaerdemaeker, T.; Wienk, M. M.; Janssen, R. A. J.; Bäuerle, P. *Angew. Chem., Int. Ed.* **2007**, *46*, 1679–1683. (g) Lo, S.-C.; Burn, P. L. *Chem. Rev.* **2007**, *107*, 1097–1116. (h) Xu, T.; Lu, R.; Liu, X.; Zheng, X.; Qiu, X.; Zhao, Y. *Org. Lett.* **2007**, *9*, 797–800. (i) Köse, M. E.; Mitchell, W. J.; Kopidakis, N.; Chang, C. H.; Shaheen, S. E.; Kim, K.; Rumbles, G. *J. Am. Chem. Soc.* **2007**, *129*, 14257–14270.

(5) (a) Xu, Z.; Moore, J. S. *Angew. Chem., Int. Ed. Engl.* **1993**, *32*, 1354–1357. (b) Andreitchenko, E. V.; Clark, C. G., Jr.; Bauer, R. E.; Lieser, G.; Müllen, K. *Angew. Chem., Int. Ed.* **2005**, *44*, 6348–6354. (c) Clark, C. G., Jr.; Wenzel, R. J.; Andreitchenko, E. V.; Steffen, W.; Zenobi, R.; Müllen, K. *J. Am. Chem. Soc.* **2007**, *129*, 3292–3301.

(6) Kopelman, R.; Shortreed, M.; Shi, Z.-Y.; Tan, W.; Xu, Z.; Moore, J. S.; Bar-Haim, A.; Klafter, J. *Phys. Rev. Lett.* **1997**, *78*, 1239–1242.

(7) (a) Sato, T.; Jiang, D.-L.; Aida, T. *J. Am. Chem. Soc.* **1999**, *121*, 10658–10659. (b) Gust, D.; Moore, T. A.; Moore, A. L. *Acc. Chem. Res.* **2001**, *34*, 40–48. (c) Nantalaksakul, A.; Reddy, D. R.; Bardeen, C. J.; Thayumanavan, S. *Photosynth. Res.* **2006**, *87*, 133–142.

(8) (a) Jiang, D. L.; Aida, T. *Nature (London, U.K.)* **1997**, *388*, 454–456. (b) Balzani, V.; Campagna, S.; Denti, G.; Juris, A.; Serroni, S.; Venturi, M. *Acc. Chem. Res.* **1998**, *31*, 26–34. (c) Gilat, S. L.; Adronov, A.; Fréchet, J. M. J. *Angew. Chem., Int. Ed.* **1999**, *38*, 1422–1427. (d) Adronov, A.; Fréchet, J. M. J. *Chem. Commun. (Cambridge, U.K.)* **2000**, 1701–1710. (e) Weil, T.; Reuther, E.; Müllen, K. *Angew. Chem., Int. Ed.* **2002**, *41*, 1900–1904. (f) Liu, D.; De Feyter, S.; Cotlet, M.; Stefan, A.; Wiesler, U.-M.; Herrmann, A.; Grebel-Koehler, D.; Qu, J.; Müllen, K.; De Schryver, F. C. *Macromolecules* **2003**, *36*, 5918–5925. (g) Thomas, K. R. J.; Thompson, A. L.; Sivakumar, A. V.; Bardeen, C. J.; Thayumanavan, S. *J. Am. Chem. Soc.* **2005**, *127*, 373–383. (h) Cotlet, M.; Vosch, T.; Habuchi, S.; Weil, T.; Müllen, K.; Hofkens, J.; De Schryver, F. *J. Am. Chem. Soc.* **2005**, *127*, 9760–9768. (i) De Schryver, F. C.; Vosch, T.; Cotlet, M.; Van der Auweraer, M.; Müllen, K.; Hofkens, J. *Acc. Chem. Res.* **2005**, *38*, 514–522. (j) Kwon, T.-H.; Kim, M. K.; Kwon, J.; Shin, D.-Y.; Park, S. J.; Lee, C.-L.; Kim, J.-J.; Hong, J.-I. *Chem. Mater.* **2007**, *19*, 3673–3680.

(9) (a) Xu, Z.; Moore, J. S. *Acta Polym.* **1994**, *45*, 83–87. (b) Xu, Z.; Kyan, B.; Moore, J. S. In *Advances in Dendritic Macromolecules*; Newkome, G. R., Ed.; JAI Press: Greenwich, CT, 1994; Vol. 1, pp 69−104. (c) Bharathi, P.;; Patel, U.;; Kawaguchi, T.;; Pesak, D. J.;; Moore, J. S. *Macromolecules* **1995**, *28*, 5955–5963. (d) Devadoss, C.; Bharathi, P.; Moore, J. S. *J. Am. Chem. Soc.* **1996**, *118*, 9635–9644. (e) Moore, J. S. *Acc. Chem. Res.* **1997**, *30*, 402–413. (f) Shortreed, M. R.; Swallen, S. F.; Shi, Z.-Y.; Tan, W.; Xu, Z.; Devadoss, C.; Moore, J. S.; Kopelman, R. *J. Phys. Chem. B* **1997**, *101*, 6318–6322. (g) Peng, Z.; Pan, Y.; Xu, B.; Zhang, J. *J. Am. Chem. Soc.* **2000**, *122*, 6619–6623. (h) Melinger, J. S.; Pan, Y.; Kleiman, V. D.; Peng, Z.; Davis, B. L.; McMorrow, D.; Lu, M. *J. Am. Chem. Soc.* **2002**, *124*, 12002–12012. (i) Pan, Y.; Lu, M.; Peng, Z.; Melinger, J. S. *J. Org. Chem.* **2003**, *68*, 6952–6958. (j) Atas, E.; Peng, Z.; Kleiman, V. D. *J. Phys. Chem. B* **2005**, *109*, 13553–13560.

(10) (a) Tour, J. M. *Chem. Rev.* **1996**, *96*, 537–553. (b) Samuel, I. D. W.; Ledoux, I.; Delporte, C.; Pearson, D. L.; Tour, J. M. *Chem. Mater.* **1996**, *8*, 819–821. (c) Pearson, D. L.; Tour, J. M. *J. Org. Chem.* **1997**, *62*, 1376–1387. (d) Tour, J. M. *Acc. Chem. Res.* **2000**, *33*, 791–804. (e) Otsubo, T.; Aso, Y.; Takimiya, K. *Bull. Chem. Soc. Jpn.* **2001**, *74*, 1789–1801. (f) Obara, Y.; Takimiya, K.; Aso, Y.; Otsubo, T. *Tetrahedron Lett.* **2001**, *42*, 6877–6881.

(11) Wu, R.; Schumm, J. S.; Pearson, D. L.; Tour, J. M. *J. Org. Chem.* **1996**, *61*, 6906–6921.

(12) (a) Gaab, K. M.; Thompson, A. L.; Xu, J.; Martínez, T. J.; Bardeen, C. J. *J. Am. Chem. Soc.* **2003**, *125*, 9288–9289. (b) Tada, T.; Nozaki, D.; Kondo, M.; Yoshizawa, K. *J. Phys. Chem. B* **2003**, *107*, 14204–14210. (c) Yuan, M.-S.; Fang, Q.; Liu, Z.-Q.; Guo, J.-P.; Chen, H.-Y.; Yu, W.-T.; Xue, G.; Liu, D.-S. *J. Org. Chem.* **2006**, *71*, 7858–7861.

(13) (a) Wang, J.-L.; Luo, J.; Liu, L.-H.; Zhou, Q.-F.; Ma, Y.; Pei, J. *Org. Lett.* **2006**, *8*, 2281–2284. (b) Jiang, Y.; Lu, Y.-X.; Cui, Y.-X.; Zhou, Q.-F.; Ma, Y.; Pei, J. *Org. Lett.* **2007**, *9*, 4539–4542.

Chart 1. Structures of **G0**, **G1**, and Reference Compound **1**

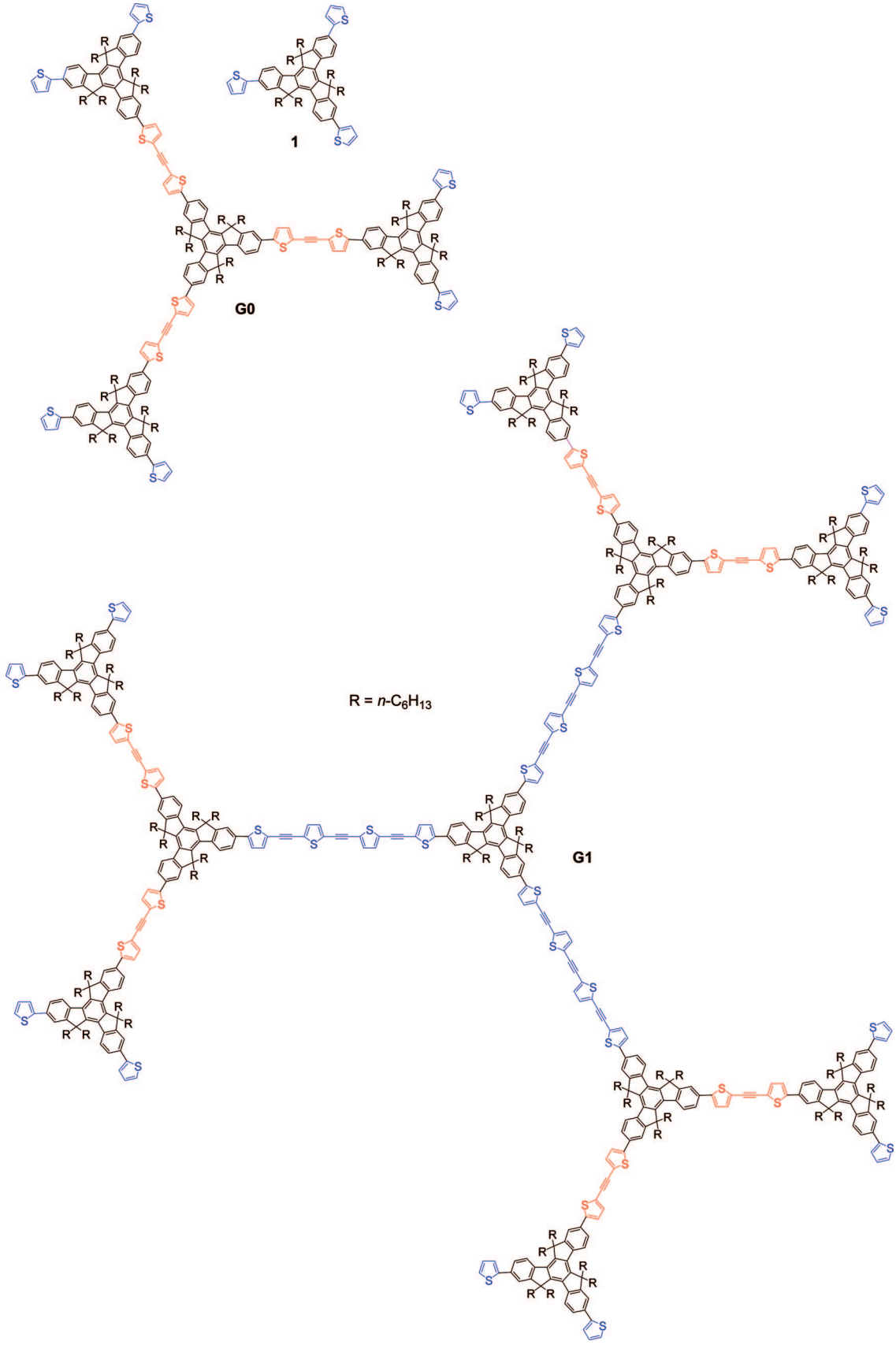

dendrimers. Herein, we wish to report (1) the synthesis of the supersized dendrimer **G2**; (2) the structural characterizations with various techniques, revealing the size and shape information of the dendrimer under different conditions; and (3) detailed studies on steady-state UV−vis absorption, photoluminescence (PL), and time-resolved fluorescence spectroscopy of **G0**−**G2**,

Chart 2. Chemical Structure of **G2**

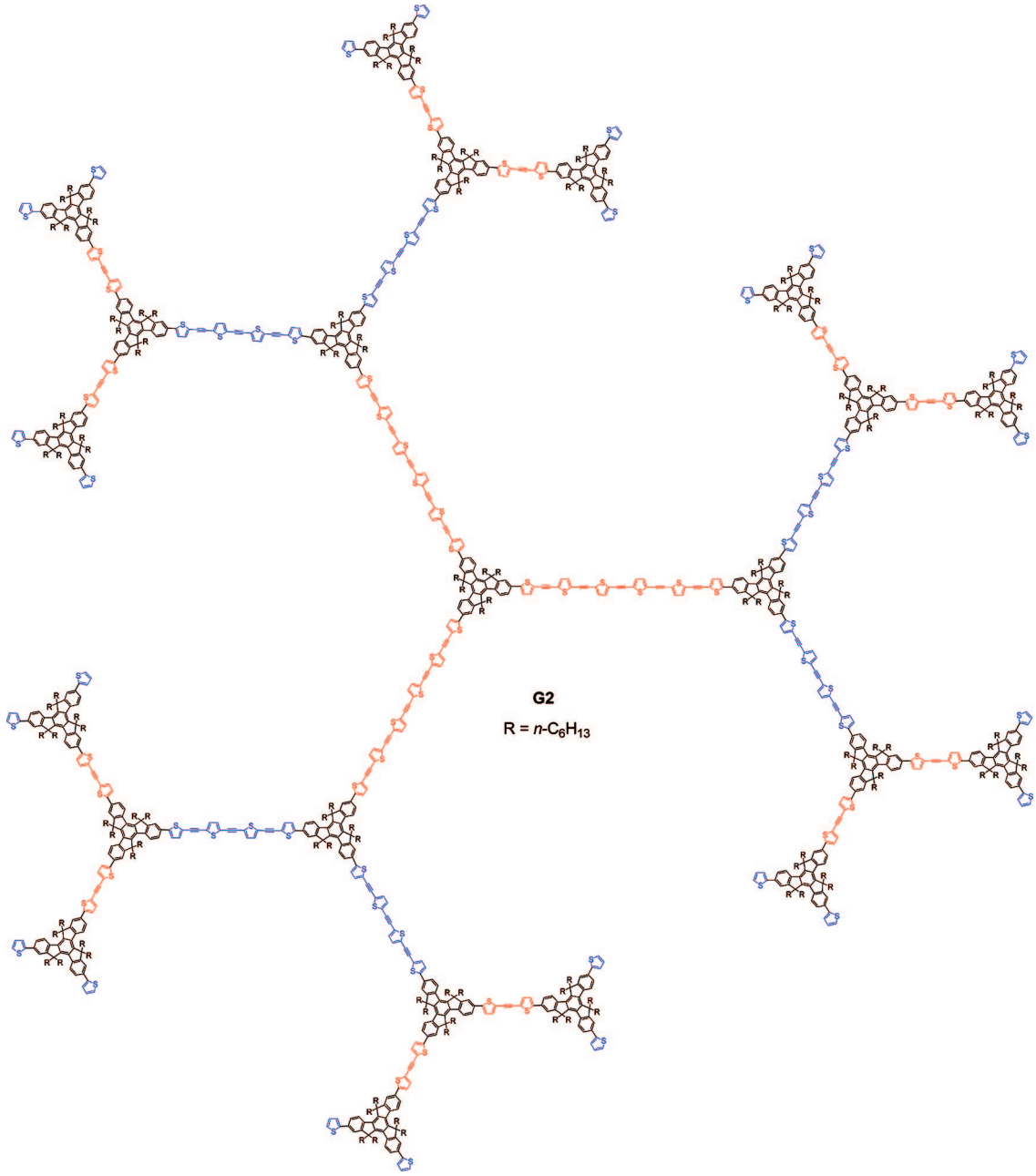

which provides insight into the photophysical properties, especially the energy transfer process, of these dendrimers.

Results and Discussion

Considering the large number of reaction steps required to synthesize **G2**, we employed a combined divergent/convergent growth approach to avoid incomplete conversion in the key reaction step.[14] Scheme 1 illustrates the synthetic approach to dendrimer **G2**. The key component in the synthesis of **G2** is the masked AB_2 building block **3**, in which A represents an acetylene moiety with a 1-hydroxy-1-methylethyl protecting group and B is the aromatic iodide group. To obtain such an AB_2 intermediate, a Sonogashira reaction between **2**[13] and 2-methylbut-3-yn-2-ol (less than 1 equiv) catalyzed by $Pd(PPh_3)_2Cl_2$ was carried out to afford **3** in 28% isolated yield, while unreacted **2** was recovered and recycled. The introduction of the polar 1-hydroxy-1-methylethyl protecting group greatly simplified the product purification by column chromatography in this step. However, the Sonogashira reaction between **3** and **4**[13] catalyzed by $Pd(PPh_3)_2Cl_2$ afforded **5** in poor yield. After the more active catalyst $Pd_2(dba)_3$[5a] and a prolonged reaction time were employed, the yield was improved to 56%. Removal of the protective group of **5** was performed in refluxing toluene under basic conditions to give dendron **6** in 51% yield. Great difficulty was encountered in the preparation of the giant dendrimer **G2** through Sonogashira cross-coupling between **2** and **6**. Typical combinations of palladium catalysts and ligands

(14) (a) Newkome, G. R.; Moorefield, C. N.; Vögtle, F. In *Dendritic Molecules: Concepts, Syntheses, and Perspectives*; VCH: Weinheim, Germany, 1996. (b) Zeng, F.; Zimmerman, S. C. *Chem. Rev.* **1997**, *97*, 1681–1712. (c) Tomalia, D. A.; Fréchet, J. M. J. In *Dendrimers and Other Dendritic Polymers*; J. Wiley and Sons Ltd.: Chichester, U.K., 2001; pp 1−44.

Scheme 1. Synthetic Route to **G2**

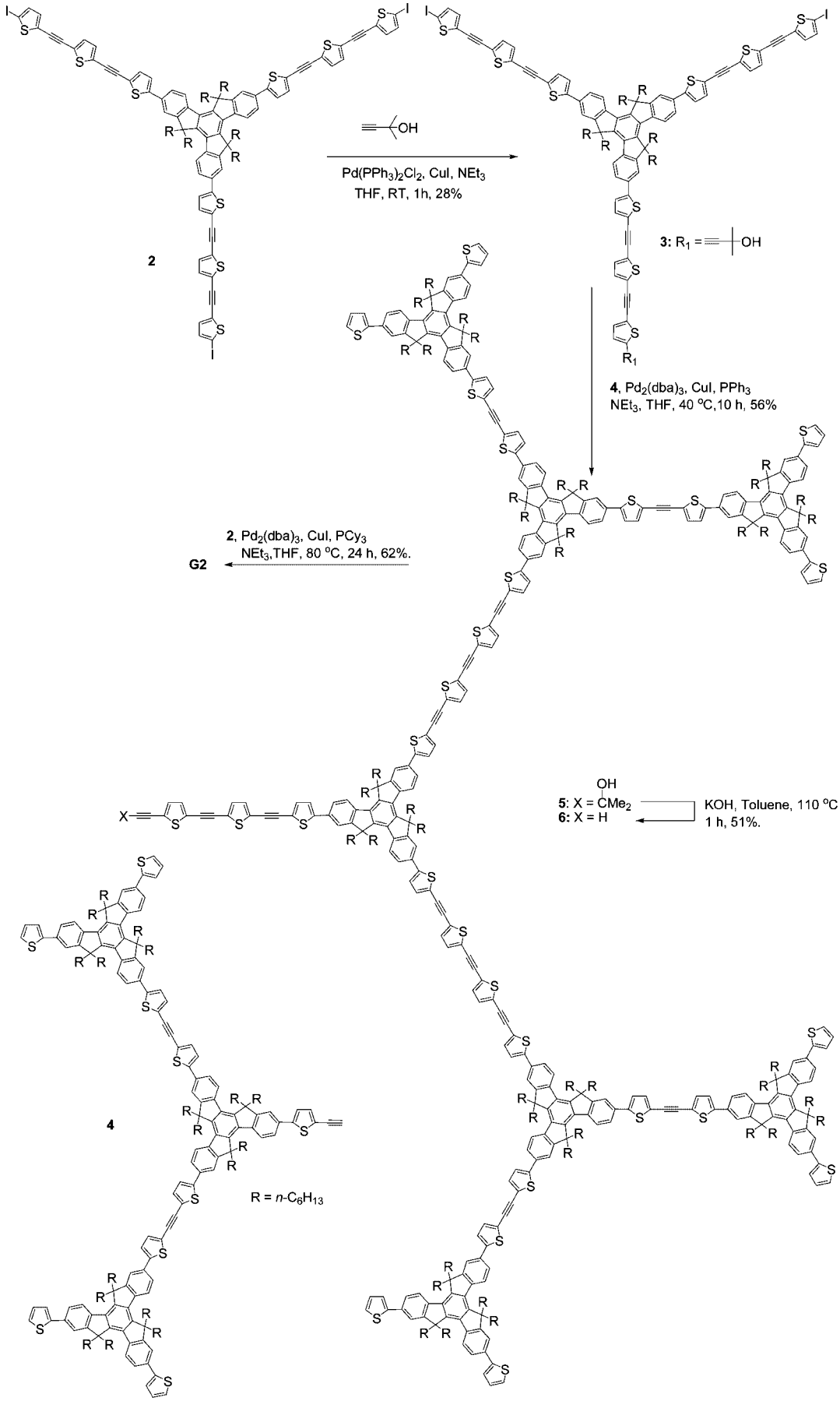

Chart 3. Structures of Model Compounds **G0m**, **G1m**, and **G2m**

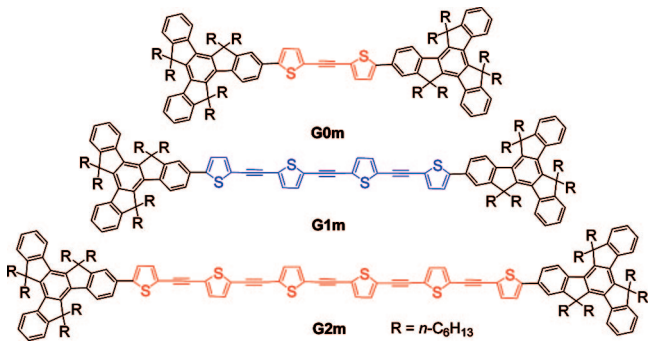

such as $Pd(PPh_3)_2Cl_2/PPh_3$, $Pd(PPh_3)_4$, or $Pd_2(dba)_3/PPh_3$ did not yield the target molecule (the only obtained product is the homodimerization product of **6**). Finally, PCy_3 was employed to suppress undesired homodimerization,[15] and the reaction temperature was increased from 40 to 80 °C. Under these conditions, convergent Sonogashira coupling between **2** and **6** afforded **G2** in 62% isolated yield, which was fairly acceptable considering the size of the produced dendrimer.

To better understand the energy transfer process within the conjugated dendrimers, the longest branch units of respective dendrimers, **G0m**, **G1m**, and **G2m** (as shown in Chart 3), also were synthesized as model compounds.[16]

As we anticipated, all compounds were readily soluble in common organic solvents, such as $CHCl_3$, THF, and toluene, owing to the large number of hexyl groups of the truxene units. All compounds were purified by silica gel chromatography, and their structures were verified by ^1H and ^{13}C NMR (see Supporting Information; Figure S1 also displays all thienyl protons of **G0**, **G1**, and **G2** in the aromatic region), elemental analysis, and MALDI-TOF MS. Figure 1 shows the MALDI-TOF MS spectrum of **G2**, in which the sharp molecular ion peak at m/z = 27 024 Da (calcd m/z = 27 072 Da) clearly indicated the molecular identity of **G2**. Neither the molecular ion peak of the side product with two arms (calcd m/z = 18 710 Da) nor that of the homodimerization impurity (calcd m/z = 16 896 Da) was observed.

Energy minimization was performed on all dendrimers using the UFF method.[17] According to the optimized conformations of the dendrimers, they assume a relatively flat shape instead of the globular shape of conventional dendrimers. The maximum radii (determined from the core to the end of fully extended periphery thiophene groups) were 3.1 nm for **G0**, 5.7 nm for **G1**, and 9.6 nm for **G2**, respectively (see Supporting Information). In Figure 2, the maximum radii of these dendrimers are compared to those of our previously reported dendrimers constructed solely from truxene units,[13b] which clearly shows the more rapid increase in molecular size of the extended dendrimers **G0**, **G1**, and **G2**. For example, the radius of giant dendrimer **G2** was 140% larger than that of corresponding **G2'** (with a radius of 4.0 nm according to molecular modeling).

To further confirm the chemical identity of the **G2** molecule as well as its molecular shape and size, we employed tapping mode AFM to investigate the **G2** molecule on mica substrates.[18] The sample was prepared by dipping the mica substrates into a

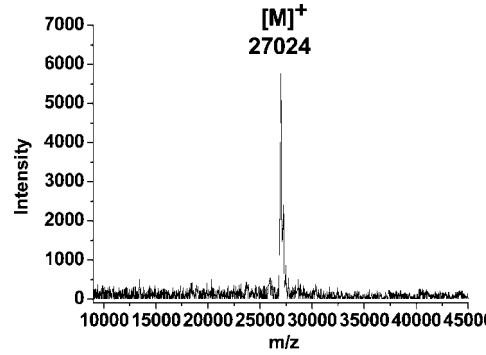

Figure 1. MALDI-TOF mass spectrum of **G2**.

$CHCl_3$ solution of **G2** at different concentrations. Figure 3 shows the AFM image of **G2** on a mica surface from a 3 nM solution. Many separated and randomly deposited spots were observed. It is noteworthy that these spots were relatively uniform in width, regardless of their heights. Although the lateral resolusion of AFM does not allow us to determine the molecular radius accurately, the uniformity in size of the observed spots leads us to speculate that they correspond to individual molecules of **G2**. The height of the spots varies in the range of 1.5−2.2 nm. The height is in fair agreement with the molecular thickness, estimated either from the molecular model or the single crystal structure of **1**[19] (see Supporting Information). This fact confirmed our initial molecular design: the use of OTEs with increasing lengths as branching units alleviates the overall steric crowdedness of **G2**, which consequently takes a comparatively flat shape rather than a globular structure (like our previously synthesized dendrimers constructed solely with truxenes). The slight deviation in height could be due to the flexibility of the hexyl chains; alternatively, the molecule might adhere to the surface with different parts of the overall structure.[5c] When the dendrimer solution was diluted to 0.3 nM and the same sample preparation procedure was performed, less spots were observed in the same area of the AFM image. However, their sizes and height distribution remained the same, which further supports our speculation that **G2** laid on the substrate as an individual molecule (see Supporting Information). In contrast, when the concentration increased to 0.3 μM, strong aggregation was observed. The size of the observed spots was ∼100 nm, with a height of ∼10 nm (see Supporting Information). This is not a surprise considering the hydrophobic nature of the molecule, which may cause the molecules to aggregate on the relatively hydrophilic surface of mica to minimize contact with the surface.

To see as to whether the shape information obtained by AFM was in fact due to the substrate−molecule interaction, as well as to study the molecular shape and size of these dendrimers in solution, dynamic light scattering experiments were performed (THF as the solvent).[20] The obtained diffusion coefficients were 2.0×10^{-10} m^2/s for **G0**, 1.1×10^{-10} m^2/s for **G1**, and 7.0×10^{-11} m^2/s for **G2**, respectively. An oblate spheroid model was

(15) Chinchilla, R.; Nájera, C. *Chem. Rev.* **2007**, *107*, 874–922.
(16) Wang, J.-L.; Tang, Z.-M.; Xiao, Q.; Zhou, Q.-F.; Ma, Y.; Pei, J. *Org. Lett.* **2008**, *10*, 17–20.
(17) Frisch, M. J.; et al. *Gaussian 03*, revision B.05; Gaussian, Inc.: Pittsburgh, PA, 2003.
(18) (a) Higuchi, M.; Shi, S.; Ariga, K.; Yamamoto, K. *J. Am. Chem. Soc.* **2001**, *123*, 4414–4420. (b) Liu, D.; Zhang, H.; Grim, P. C. M.; De Feyter, S.; Wiesler, U.-M.; Berresheim, A. J.; Müllen, K.; De Schryver, F. C. *Langmuir* **2002**, *18*, 2385–2391.
(19) (a) Pei, J.; Wang, J.-L.; Cao, X.-Y.; Zhou, X.-H.; Zhang, W.-B. *J. Am. Chem. Soc.* **2003**, *125*, 9944–9945. (b) Sun, Y.; Xiao, K.; Liu, Y.; Wang, J.-L.; Pei, J.; Yu, G.; Zhu, D. *Adv. Funct. Mater.* **2005**, *15*, 818–822. (c) Wang, J.-L.; Duan, X.-F.; Jiang, B.; Gan, L.-B.; Pei, J.; He, C.; Li, Y.-F. *J. Org. Chem.* **2006**, *71*, 4400–4410.

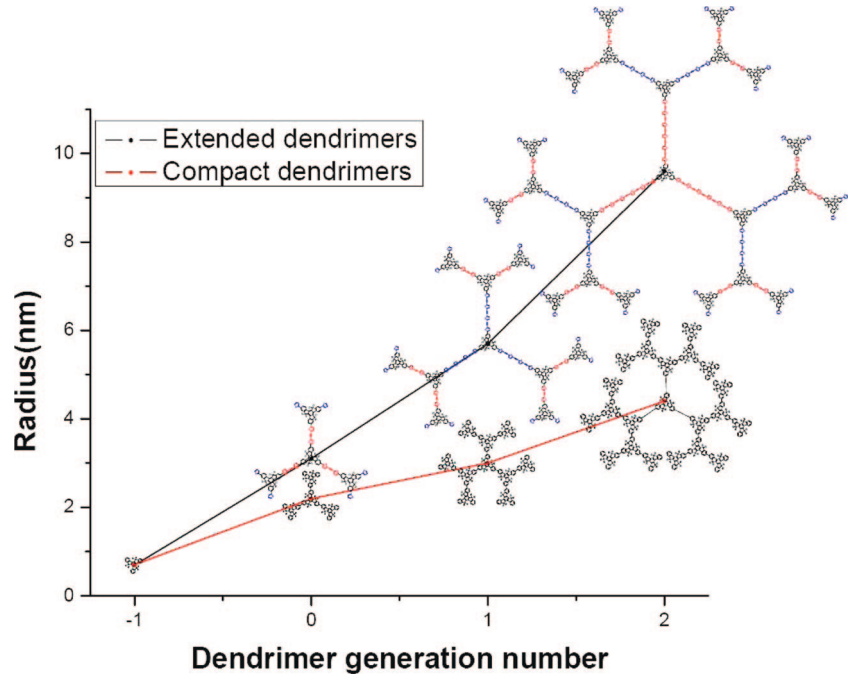

Figure 2. Comparison between radii of dendrimers **G0**−**G2** and radii of dendrimers solely comprised of truxene **G0**'−**G2**' (a single truxene unit also was incorporated to indicate the same origin of the two series of dendrimers).

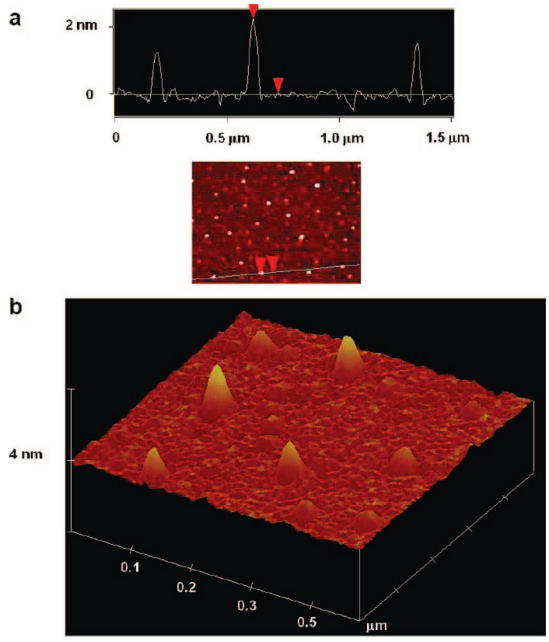

Figure 3. (a) AFM images and height profiles of the individual dendrimer **G2** molecule on mica from a 3 nM solution. (b) 3-D AFM images of the individual dendrimer **G2** molecule on mica from a 3 nM solution.

applied to calculate the molecular radius (see Supporting Information). The *b* value in the equation was set to 1.6 nm, based on the calculation result and the crystal structure of **1**. Thus, a radius of 2.7 nm was obtained for **G0**, 5.7 nm for **G1**, and 9.7 nm for **G2**, respectively. These results were very close to the radii obtained from molecular modeling (e.g., a difference of ca. 1% for **G2**), which again confirmed the flat shape and large radii of our shape-persistent conjugated dendrimers. GPC results also showed an increase in the molecular size from **G0** to **G2**, as shown in Figure S12.

The photophysical properties of all dendrimers and model compounds were investigated to understand their energy transfer properties. Photophysical data from both solution and thin films are summarized in Table 1. The absorption and PL spectra in dilute THF solutions (ca. 10^{-7} M) are shown in Figures 4 and 5. The absorption spectra of the dendrimers showed two distinct absorption bands. The absorption peak at ~343 nm was assigned to the periphery unit (part of **1**) in all these dendrimers.[19] Upon increasing the dendrimer generation, the molar extinction coefficient of this absorption peak increased dramatically, which is consistent with the increase of the number of periphery units in the dendrimer. Also, the dendrimers exhibited another absorption peak at 398 nm for **G0** (394 nm for **G0m**), 410 nm for **G1** (416 nm for **G1m**), and 414 nm for **G2** (424 nm for **G2m**), respectively.[16] The 10 nm blue shift of the absorption peak of **G2** as compared to that of the linear model compound **G2m** can be explained by considering the structure of dendrimer **G2** as being constructed from a combination of 3 **G2m** units, 6 **G1m** units, and 12 **G0m** units. Because of the high absorbance in the short wave region, this combination shifts the apparent absorption maximum of **G2** toward the short wavelengths.[21] All these molecules have fairly large molar extinction coefficients at their absorption maxima. **G2** has an especially high molar extinction coefficient value (9.6×10^6 M^{-1} cm^{-1}) at 414 nm, as compared to that of the reference compound **G2m** (1.5×10^5 M^{-1} cm^{-1}) at 424 nm. The effective conjugation length was extended steadily with increasing dendrimer generation, due to the incorporation of longer chromophores. A comparison of the unsubstituted OTEs (with λ_{max} values of 317 and 377 nm for $n = 2$ and 4) with **G0** and **G1** revealed that the terminal

(20) (a) Liao, L.-X.; Stellacci, F.; McGrath, D. V. *J. Am. Chem. Soc.* **2004**, *126*, 2181–2185. (b) Newkome, G. R.; Wang, P.; Moorefield, C. N.; Cho, T. J.; Mohapatra, P. P.; Li, S.; Hwang, S.-H.; Lukoyanova, O.; Echegoyen, L.; Palagallo, J. A.; Lancu, V.; Hla, S.-W. *Science (Washington, DC, U.S.)* **2006**, *312*, 1782–1785.
(21) Ramakrishna, G.; Bhaskar, A.; Bäuerle, P.; Goodson, T., III. *J. Phys. Chem. A* **2008**, *112*, 2018–2026.

Table 1. Photophysical Data of All Compounds Both in Dilute THF Solutions and in Thin Films

compound	absorption[a] λ_{max}(nm soln (log ε))	absorption[b] λ_{max}(nm films)	emission[a] λ_{max}(nm soln)	emission[b] λ_{max}(nm films)	Φ_{PL}[c] (%)	τ (ns)[d] (χ^2)
1	343 (5.26)	343	380	382		6.08 (1.04)
		362	397	400		
	343 (6.04)	345	460	508		0.41 (94.4%)
G0	355 (6.00)	357	490		29	6.17 (5.6%)
	398 (5.98)	402				(1.12)
G0m[16]	308 (4.92)	309	460	470	25	0.42 (91.4%)
	394 (4.99)	400	487	491		1.29 (8.6%) (1.08)
	343 (6.36)	346	484	521		0.31 (97.3%)
G1	355 (6.38)	358	511		23	3.07 (2.7%)
	410 (6.43)	404				(1.12)
G1m[16]	308 (4.92)	309	484	525	20	0.32 (84.3%)
	416 (5.08)	415	512			1.50 (15.7%) (1.16)
	343 (6.76)	347	490	548	19	0.31 (95.8%)
G2	355 (6.75)	359	515			1.91 (4.2%)
	414 (6.98)	404				(1.30)
G2m[16]	308 (4.92)	309	490	515	18	0.31 (98.2%)
	424 (5.15)	424	516			1.64 (1.8%) (0.99)

[a] In THF solution (10^{-7} M). [b] In thin films. [c] In THF solution ($A = 0.1$) and 9,10-diphenylanthracene as standard. [d] In THF solution (10^{-7} M), the fluorescence decay was monitored at the maximum emission peak. Time-resolved fluorescence of all compounds except **1** shows biexponential decay. The percentage in parentheses indicates the contribution from each lifetime component. All emission spectra except that of **1** (at 343 nm) were collected when excited at 372 nm.

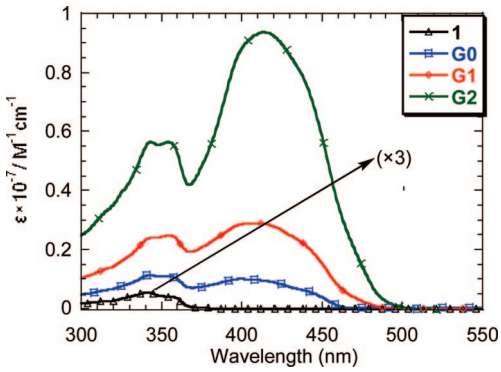

Figure 4. Absorption spectra of dendrimers **G0**−**G2** and **1** in THF solution (10^{-7} M) at room temperature.

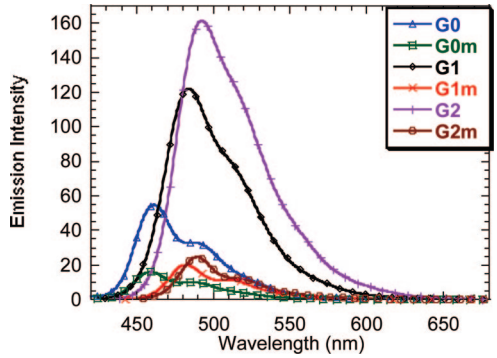

Figure 5. Emission spectra of dendrimers and reference compounds in THF solutions (10^{-7} M) at room temperature. All emission spectra were collected with an excitation wavelength at the absorption maxima of longer wavelengths of the corresponding compounds.

truxene moiety participated in the conjugated system and thus induced a red shift.[22] The absorption peaks of **G2** and **G2m** almost approach that of poly(2,5-thienylethynylene) (~433 nm).[10c] This observation is consistent with previous research results that the maximum effective conjugation length of OTEs occurs at the octamer.[23] The excitation spectra of both dendrimers also were similar to their absorption spectra (for the result of **G2**, see Figure S14).

The emission spectra of these dendrimers and their reference compounds showed a maximum peak with a shoulder, corresponding to 0−0 and 0−1 transitions, respectively, similar to those of linear OTEs.[24] As shown in Figure 5, the emission maximum λ_{max} peaked at 460 nm for **G0**, 484 nm for **G1**, and 490 nm for **G2**, respectively. The reference compound **G0m** exhibited very similar emission features to its counterpart **G0**. Similar behaviors were observed between **G1m** and **G1** and **G2m** and **G2**. The emission maximum λ_{max} of **G1** and **G2** exhibited red shifts of 24 and 40 nm, relative to that of **G0**, due to the increase of the effective conjugation length in the branch structures with the increase of generation. The apparent Stokes shifts were 62 nm for **G0**, 74 nm for **G1**, and 76 nm for **G2**. The progressively larger Stokes shifts imply that the dendrimer backbone becomes less rigid as the molecular size grows larger. The fluorescence quantum yields (Φ_{PL}) of these dendrimers in dilute solutions were measured to be 0.29, 0.23, and 0.19 for **G0**, **G1**, and **G2**, respectively (absorbance values were ca. 0.1, and 9,10-diphenylanthracene was used as the standard). As a comparison, the fluorescence quantum yields of **G0m**, **G1m**, and **G2m** were 0.25, 0.20, and 0.18, respectively. The lower Φ_{PL} values in the higher generation dendrimer[9d] correlated well with the trend of their apparent Stokes shifts, reflecting the structural rigidity change.

The fluorescence lifetimes of the dendrimers and reference compounds were measured in THF solutions using a time-correlated photon counting instrument. The results also are shown in Table 1. The decay of the emission maximum of the model compounds (**G0m**−**G2m**) was found to be biexponential when excited at 372 nm.[25] The major lifetime component was 0.42 ns for **G0m**, 0.32 ns for **G1m**, and 0.31 ns for **G2m**,

(22) Geisler, T.; Petersen, J. C.; Bjørnholm, T.; Fischer, E.; Larsen, J.; Dehu, C.; Brédas, J.-L.; Tormos, G. V.; Nugara, P. N.; Cava, M. P.; Metzger, R. M. *J. Phys. Chem.* **1994**, *98*, 10102–10111.

(23) (a) Melucci, M.; Barbarella, G.; Zambianchi, M.; Di Pietro, P.; Bongini, A. *J. Org. Chem.* **2004**, *69*, 4821–4828. (b) Meier, H.; Mühling, B.; Oehlhof, A.; Theisinger, S.; Kirsten, E. *Eur. J. Org. Chem.* **2006**, *62*, 405–413.

(24) Nakao, K.; Nishimura, M.; Tamachi, T.; Kuwatani, Y.; Miyasaka, H.; Nishinaga, T.; Lyoda, M. *J. Am. Chem. Soc.* **2006**, *128*, 16740–16747.

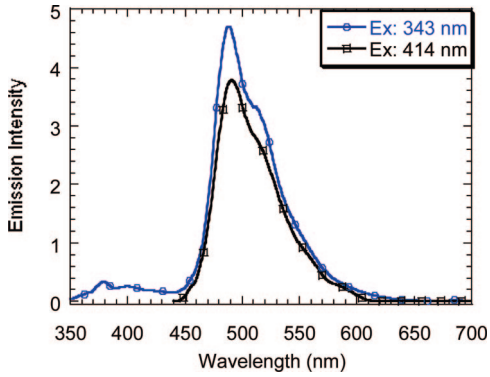

Figure 6. Emission spectra of **G2** recorded at different excitation wavelengths in THF solution (3×10^{-9} M) at room temperature.

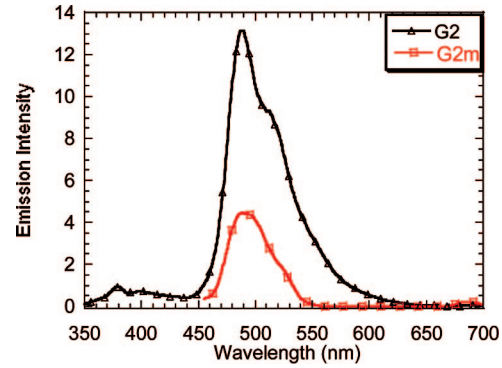

Figure 7. Emission spectra of **G2** (10^{-8} M) and **G2m** (3×10^{-8} M) excited at 343 nm in THF solution.

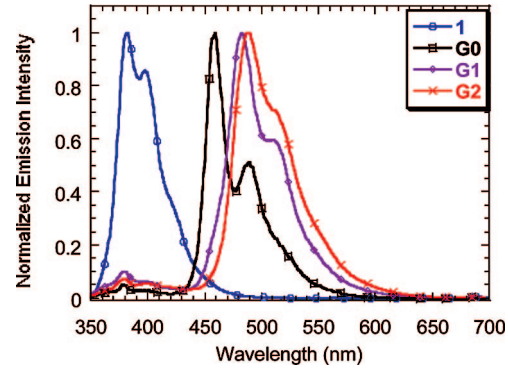

Figure 8. Comparison of emission spectra of dendrimers in THF solution excited at 343 nm (3×10^{-9} M).

respectively. Another component with a relatively small contribution exhibited a longer lifetime ranging from 1.29 to 1.64 ns. Similarly, the emission maximum band decays of dendrimers **G0**−**G2** also were fitted by biexponential decays. The lifetimes with greater contributions were 0.41 ns for **G0** and 0.32 ns for **G1** and **G2**, almost identical to those derived from their corresponding model compounds. These facts suggest an energy cascade process in which the final emission came from the longest conjugated chromophores with the smallest energy gap, as discussed in detail in the next paragraph.

Our shape-persistent dendrimers represent an ideal platform to study the intramolecular energy transfer process. As shown in Figure 6, when **G2** was excited at 343 nm where the absorption of the dendrimer terminal units dominates, the emission came almost exclusively from the longest branch units. The residual fluorescence from the unit **1** chromophore in the range between 380 and 400 nm became very weak. This behavior, again, indicates a highly efficient intramolecular energy transfer process from the shorter chromophores at the periphery to the longer ones in the interior. Moreover, despite their similar PL quantum yields when excited at the absorption maxima of longer wavelengths, the emission intensity of **G2** was several times higher than that of model **G2m** when both were excited at 343 nm at the same concentration of the longest branch, which clearly showed an antenna effect (Figure 7). At this time, it was not clear as to whether a mechanism of multistep hopping of the exciton among different branching units was involved or if the light energy absorbed by the periphery was directly transferred to the core. However, a Förster resonance energy transfer mechanism can be assumed for our dendrimers for two reasons.[9,26] First, as stated previously, the electronic communication among chromophores joined by the same truxene unit was very small,[12] similar to the case in meta-substituted benzene. This fact greatly diminishes the possibility of a Dexter exchange mechanism, in which orbital overlap is usually necessary. Second, the emission spectrum of the peripheral unit has a large overlap with the absorption spectrum of **G2m**, which is ideal for resonant excitation energy transfer via dipole−dipole interactions. To quantify the energy funneling ability of our dendrimers, we measured the fluorescence quantum yields of **G0**−**G2** and **1** upon excitation at 343 nm. The energy transfer efficiency is deduced from the comparison between the fluorescence quantum efficiency of **1** to that of residual emission between 350−450 nm in dendrimers (Figure 8).[9h] Calculated results showed that the energy transfer efficiencies were 96% for **G0**, 97% for **G1**, and 98% for **G2**, respectively. The high energy transfer efficiency can be ascribed to the large overlap between emission of the donor and absorption of the acceptor and gradient energy flow from the periphery to the core, as mentioned earlier. We noted that the efficiency of energy transfer did not decrease with increasing generation, in contrast to what was often observed for compact dendrimers.[9d] This fact shows the importance of creating an energy gradient to guide the energy transfer direction, which, from an entropic view, ought to favor exciton migration in the opposite direction.[27]

Thin films used for UV−vis and PL measurements were obtained by spin-coating of a toluene solution (ca. 5 mg/mL) onto quartz plates at 1000 rpm. All dendrimers exhibited an excellent film-forming property. This property, combined with its good thermal stability (i.e., **G2** showed only a 5% weight loss when heated to 380 °C under a nitrogen atmosphere as shown in the Supporting Information), makes our dendrimer suitable for future applications in optical and electrical devices. The absorption spectra of dendrimers in thin films were very similar to those in dilute solution, indicating that no significant intermolecular aggregation occurred in the ground states, due to the branching architecture of the dendrimers and the large number of alkyl groups.[13b] Their emission spectra in thin films

(25) (a) Rose, A.; Lugmair, C. G.; Swager, T. M. *J. Am. Chem. Soc.* **2001**, *123*, 11298–11299. (b) Wang, Y.; Ranasinghe, M. I.; Goodson, T., III. *J. Am. Chem. Soc.* **2003**, *125*, 9562–9563. (c) Ahn, T. S.; Thompson, A. L.; Bharathi, P.; Müller, A.; Bardeen, C. J. *J. Phys. Chem. B* **2006**, *110*, 19810–19819.

(26) (a) Selvin, P. R. *Nat. Struct. Biol.* **2000**, *7*, 730–734. (b) Hu, D.; Yu, J.; Wong, K.; Bagchi, B.; Rossky, P. J.; Barbara, P. F. *Nature (London, U.K.)* **2000**, *405*, 1030–1033.

(27) Swallen, S. F.; Kopelman, R.; Moore, J. S.; Devadoss, C. *J. Mol. Struct.* **1999**, *485*−*486*, 585–597.

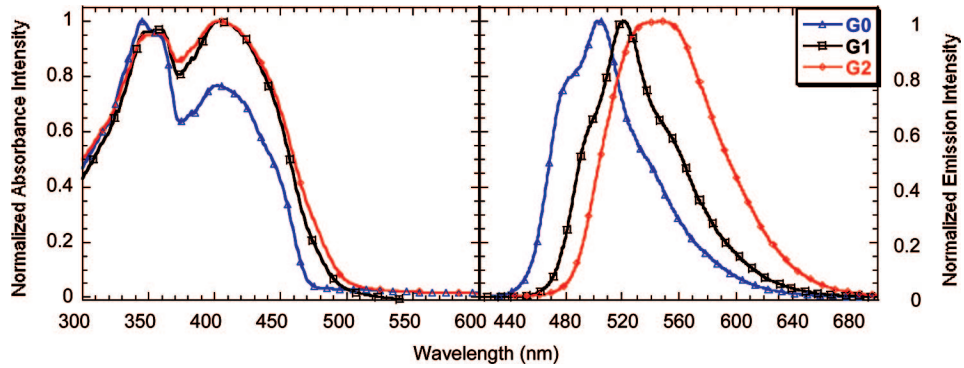

Figure 9. Comparison of absorption spectra (left) and emission spectra (right) of dendrimers in thin films. All emission spectra were collected at excitation at the absorption maximum of the corresponding compounds.

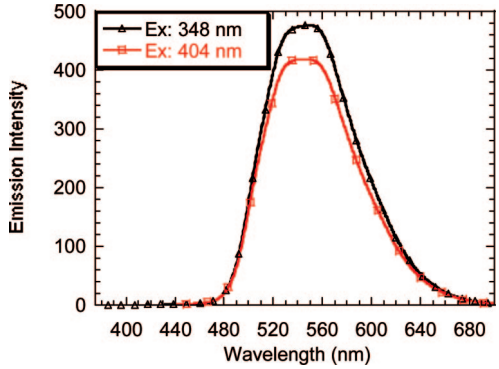

Figure 10. Comparison of emission spectra of dendrimer **G2** in thin films.

became broad and featureless (Figure 8). In comparison to those in dilute solution, the emission λ_{max} red shifted by 18 nm for **G0**, 10 nm for **G1**, and 33 nm for **G2**, indicating the formation of excimer. Moreover, the energy transfer process seemed to be more efficient in films, as the residual emission of **G2** between 350 and 450 nm present in the solution spectrum when excited at 343 nm disappeared in the emission spectrum of the film, possibly due to additional contributions from intermolecular energy transfer (Figure 10).

Conclusion

In conclusion, we successfully synthesized a supersized, shape-persistent dendrimer **G2** using a double-stage divergent/convergent growth approach. To the best of our knowledge, our super extended **G2** dendrimer, with a radius of 9.6 nm and a molecular weight of 27 072 Da, is the largest one among thus reported second generation dendrimers. We confirmed the molecular size as well as its relative flat shape both on the substrate and in solution by AFM and DLS techniques, respectively. The energy gradient in **G2**, which is pivotal in the directional energy transfer process, was engineered by linking chromophore units of increasing effective conjugation lengths in the direction from the dendritic rim to the core. Detailed investigations on steady-state UV−vis absorption and PL as well as time-resolved fluorescence spectroscopy of these dendrimers provide insight into the photophysical process in such dendrimers. Our gradient, shape-persistent dendrimers show an excellent energy funneling ability, evidenced by their high energy transfer efficiency. Also, we note that the energy transfer efficiency does not decrease with increasing generation, stressing the importance of the energy gradient. A number of areas can be envisaged where our molecular-based antenna may be a promising candidate, such as light-harvesting materials, solar energy conversion materials, and organic lasers, etc. Finally, we note that our present synthetic strategy allows further functionalization at the periphery of the dendrimers, which can be tuned according to different applications.

Experimental Section

Compound 3. To a solution of **2** (1.1 g, 0.51 mmol) in anhydrous THF (10 mL) was added a mixture of $Pd(PPh_3)_2Cl_2$ (17 mg, 0.025 mmol), CuI (4.7 mg, 0.025 mmol), and 2-methylbut-3-yn-2-ol (38 mg, 0.45 mmol) in anhydrous THF (50 mL). Five milliliters of Et_3N was added dropwise to the mixture. After 1 h at room temperature, the mixture was poured into water. The aqueous layer was extracted with EtOAc, and the organic extracts were washed with brine and water and then dried over $MgSO_4$. After removal of solvents under reduced pressure, the residue was purified by flash column chromatography (petroleum ether/EtOAc, 5:1) to provide **3** as a yellow solid (0.29 g, 28%). ^{1}H NMR ($CDCl_3$, 400 MHz, ppm): δ 8.37−8.39 (d, J = 8.4 Hz, 3H, Ar−H), 7.67−7.69 (m, 6H, Ar−H), 7.38−7.39 (d, J = 3.6 Hz, 3H, Ar−H), 7.34−7.35 (d, J = 3.6 Hz, 3H, Ar−H), 7.17−7.19 (m, 8H, Ar−H), 7.14−7.15 (d, J = 3.6 Hz, 1H, Ar−H), 7.07−7.08 (d, J = 3.6 Hz, 1H, Ar−H), 6.96−6.97 (d, J = 3.6 Hz, 2H, Ar−H), 2.95−2.97 (m, 6H, CH_2), 2.05−2.12 (m, 6H, CH_2), 2.01 (s, 1H, OH), 1.65 (s, 6H, CH_3), 0.84−0.95 (m, 36H, CH_2), 0.55−0.62 (m, 30H, CH_2, CH_3). ^{13}C NMR ($CDCl_3$, 100 MHz, ppm): δ 154.5, 147.2, 145.5, 140.3, 137.9, 137.2, 133.8, 133.7, 132.4, 132.3, 132.2, 132.0, 131.9, 131.7, 128.6, 125.1, 125.0, 124.8, 124.2, 124.1, 124.0, 123.6, 123.1, 121.2, 119.2, 98.8, 88.2, 87.7, 87.1, 86.67, 86.65, 86.2, 77.2, 75.7, 75.0, 65.8, 55.8, 37.0, 31.4, 31.2, 29.4, 23.9, 22.2, 13.8. MALDI-TOF MS (m/z): calcd for $C_{116}H_{112}I_2OS_9$: 2063.4; found: 2063.6 (M^+). Elemental analysis: calcd for $C_{116}H_{112}I_2OS_9$: C, 67.48; H, 5.47; found: C, 66.95; H, 5.78.

Compound 5. To a mixture of **3** (0.65 g, 0.31 mmol), **4** (2.2 g, 0.66 mmol), $Pd_2(dba)_3$ (14 mg, 0.015 mmol), PPh_3 (20 mg, 0.075 mmol), and CuI (3.0 mg, 0.015 mmol) in anhydrous THF (20 mL) was added 40 mL of Et_3N. The mixture was stirred at 40 °C under nitrogen atmosphere. After 10 h, the mixture was poured into water, and the aqueous layer was extracted with dichloromethane. The combined organic extracts were washed with brine and water and then dried over $MgSO_4$. After removal of solvents under reduced pressure, the residue was purified by flash column chromatography (petroleum ether/EtOAc, 5:1) to afford **5** as a red solid (1.43 g, yield: 56%). ^{1}H NMR ($CDCl_3$, 400 MHz, ppm): δ 8.29−8.31 (m, 21H, Ar−H), 7.61−7.63 (m, 42H, Ar−H), 7.40−7.41 (d, J = 3.6 Hz, 9H, Ar−H), 7.31−7.35 (m, 12H, Ar−H), 7.25−7.29 (m, 17H, Ar−H), 7.12−7.16 (m, 8H, Ar−H), 7.07−7.10 (m, 11H, Ar−H), 7.05−7.07 (m, 4H, Ar−H), 7.00−7.05 (d, J = 3.6 Hz, 1H, Ar−H), 2.90−2.97 (m, 42H, CH_2), 2.06−2.07 (m, s, 43H, CH_2, OH), 1.48 (s, 6H, CH_3), 0.78−0.90 (m, 252H, CH_2), 0.51−0.56 (m, 210H,

CH_2, CH_3). ^{13}C NMR ($CDCl_3$, 100 MHz, ppm): δ 154.55, 154.52, 154.47, 154.39, 154.36, 147.3, 147.2, 146.8, 146.7, 145.5, 145.4, 145.3, 145.21, 145.18, 145.1, 144.88, 144.86, 143.6, 143.5, 141.8, 141.7, 140.44, 140.33, 139.98, 139.72, 139.68, 139.65, 138.08, 138.04, 138.01, 137.9, 137.8, 133.8, 133.3, 132.54, 132.51, 132.47, 132.41, 132.25, 132.18, 132.01, 131.99, 131.95, 131.7, 130.9, 128.8, 128.1, 127.5, 125.10, 125.03, 124.95, 124.81, 124.6, 124.15, 124.12, 123.8, 123.7, 123.64, 123.62, 123.58, 123.1, 123.0, 122.9, 121.8, 121.7, 121.5, 121.4, 121.2, 119.3, 119.0, 98.9, 88.4, 88.3, 87.7, 87.6, 87.3, 87.1, 86.8, 86.7, 77.2, 75.0, 65.7, 55.85, 55.78, 37.1, 31.5, 31.2, 29.7, 29.6, 29.5, 24.0, 22.3, 13.9. MALDI-TOF MS (*m*/*z*): calcd for $C_{578}H_{678}OS_{27:}$ 8507.3; found: 8508 (M^+). Elemental analysis: calcd for $C_{578}H_{678}OS_{27}$: C, 81.60; H, 8.03; found: C, 81.99; H, 8.27.

Compound 6. To a solution of **5** (0.85 g, 0.10 mmol) in 150 mL of toluene was added KOH (56 mg, 1.0 mmol). The mixture was refluxed for 1 h. The solution was neutralized by an aqueous solution of NH_4Cl. The aqueous layer was extracted with dichloromethane. The combined extracts were washed with brine and dried over $MgSO_4$. After removal of the solvents under reduced pressure, the residue was purified by flash column chromatography (petroleum ether/CH_2Cl_2, 4:1) to provide **6** as a yellow solid. (0.43 g, yield: 51%) ^1H NMR ($CDCl_3$, 400 MHz, ppm): δ 8.36−8.38 (m, 21H, Ar−H), 7.69−7.71 (m, 42H, Ar−H), 7.47−7.49 (d, J = 3.6 Hz, 9H, Ar−H), 7.40−7.42 (m, 12H, Ar−H), 7.33−7.37 (m, 15H, Ar−H), 7.12−7.23 (m, 26H, Ar−H), 3.41 (s, 1H, CH), 2.98−3.01 (m, 42H, CH_2), 2.12−2.16 (m, 42H, CH_2), 0.88−0.94 (m, 252H, CH_2), 0.59−0.64 (m, 210H, CH_2, CH_3). ^{13}C NMR ($CDCl_3$, 100 MHz, ppm): δ 154.5, 154.4, 147.3, 147.2, 145.5, 145.4, 145.36, 145.32, 145.17, 145.11, 144.9, 143.6, 143.5, 141.8, 141.7, 140.4, 140.3, 139.99, 139.85, 139.7, 138.0, 137.9, 133.8, 133.0, 132.5, 132.4, 132.2, 132.0, 131.7, 128.1, 127.6, 125.1, 125.0, 124.6, 124.1, 124.02, 123.97, 123.8, 123.6, 123.1, 122.9, 121.4, 121.2, 119.3, 119.0, 88.4, 87.0, 86.82, 86.77, 82.7, 77.2, 76.4, 55.84, 55.78, 37.1, 31.5, 29.5, 24.0, 22.3, 13.9. MALDI-TOF MS (*m*/*z*): calcd for $C_{575}H_{672}S_{27:}$ 8449.2; found: 8449 (M^+). Elemental analysis: calcd. for $C_{575}H_{672}S_{27}$: C, 81.74; H, 8.02; found: C, 81.55; H, 8.27.

Compound G2. To a mixture of **6** (0.22 g, 0.026 mmol), **2** (14 mg, 0.0066 mmol), $Pd_2(dba)_3$ (1.6 mg, 0.0017 mmol), PCy_3 (1.8 mg, 0.0066 mmol), and CuI (0.3 mg, 0.0017 mmol) in anhydrous THF (10 mL) was added 20 mL of Et_3N. The mixture was stirred at 80 °C under nitrogen atmosphere. After 24 h, the mixture was poured into water, and then the aqueous layer was extracted with dichloromethane. After extraction, the combined organic layers were washed with brine and then dried over $MgSO_4$. After removal of solvents under reduced pressure, the residue was purified by flash column chromatography (petroleum ether/CH_2Cl_2, 2:1) to afford **G2** as a red solid (0.11 g, yield: 62%). ^1H NMR ($CDCl_3$, 800 MHz, ppm): δ 8.36−8.39 (m, 66H, Ar−H), 7.69 (m, 132H, Ar−H), 7.47−7.48 (d, J = 3.6 Hz, 30H, Ar−H), 7.40−7.41 (m, 48H, Ar−H), 7.35−7.36 (m, 42H, Ar−H), 7.33−7.34 (m, 30H, Ar−H), 7.20−7.23 (m, 40H, Ar−H),7.15−7.16 (dd, J = 4.8, 3.6 Hz, 24H, Ar−H), 2.97−2.98 (m, 132H, CH_2), 2.12−2.15 (m, 132H, CH_2), 0.86−0.98 (m, 792H, CH_2), 0.56−0.63 (m, 660H, CH_2, CH_3). ^{13}C NMR ($CDCl_3$, 100 MHz, ppm): δ 154.7, 154.5, 147.4, 147.0, 146.9, 145.7, 145.5, 145.4, 145.3, 145.0, 140.6, 140.4, 139.8, 138.2, 138.0, 134.0, 133.4, 132.7, 132.1, 132.0, 131.9, 128.2, 125.2, 125.1, 124.7, 124.3, 123.2, 123.1, 122.0, 121.9, 121.4, 119.4, 88.5, 87.8, 87.4, 86.9, 55.9, 37.2, 31.6, 29.6, 24.1, 22.4, 14.0. MALDI-TOF MS (*m*/*z*): calcd for $C_{1836}H_{2118}S_{90}$: 27 072; found: 27 024 (M^+). Elemental analysis: calcd for $C_{1836}H_{2118}S_{90}$: C, 81.45; H, 7.89; found: C, 80.89; H, 7.78.

Acknowledgment. This work was supported by the Major State Basic Research Development Program (2002CB613402 and 2007CB808000) from the Ministry of Science and Technology, China and the National Natural Science Foundation of China (NSFC 20425207, 50473016, 20521202, and 20604001). We thank Prof. Dahui Zhao for helpful discussions, Prof. Dehai Liang and Jingjing Yan for their help with DLS measurements, and Prof. Jiang Bian and Degao Peng for help with calculations.

Supporting Information Available: ^1H and ^{13}C NMR spectra, and MS data for all new compounds. This material is available free of charge via the Internet at http://pubs.acs.org.

JA803109R